Journal of Education and Science (ISSN 1812-125X)

www.edusj.mosuljournals.com

A Decision Support System Based on Machine Learning for Land Investment

Dhufr H. M. Alali[(1)] * Timur İnan [(2)]

[(1)] Altinbas University, *Information Technologies*, Istanbul, Turkey
[(1)] Ninavah Investment Commission, Mosul, Iraq
[(2)] Altınbaş University, *Software Engineering*, Istanbul, Turkey

Article information

Article history:
Received June 11, 2023
Accepted July 23, 2023
Available online December 01, 2023

Keywords:
Deep Learning
Transfer Learning
Aerial Photograph
Classification

Correspondence:
Dhufr Hussein Mohammed Alali
dhafar.csp82@student.uomosul.edu.iq

Abstract

This research paper proposes a methodology for classifying aerial photographs and lands using deep learning with transfer learning. The study utilizes the Aerial Image Dataset (AID), which contains a diverse set of aerial images with 30 scene classes. The proposed methodology involves data preprocessing, dataset splitting, training images, model selection, model training, and evaluation using performance measures. Three neural network models (ResNet50, VGG19, and EfficientNetB3) are compared, and the best model is selected based on performance metrics such as precision, recall, F1-score, and the confusion matrix. The results show the effectiveness of the proposed methodology in accurately classifying aerial photographs. This indicates that EfficientNetB3 has a higher ability to classify aerial photographs and lands compared to ResNet50 and VGG19. ResNet50 achieved moderate performance with relatively lower precision, recall, and F1-score compared to EfficientNetB3. VGG19, on the other hand, demonstrated the lowest performance across all metrics, showing low precision, recall, and F1-score values. These results can contribute to various applications such as urban planning, real estate development, and land management.

DOI: 10.33899/edusj.2023.141005.1375, ©Authors, 2023, College of Education for Pure Science, University of Mosul.

1.Introduction

Land investments encompass various common types, including residential and commercial development land, cropland and livestock-raising land, mineral production land, and recreational land [1][2]. There are several factors to consider when investing in land. These include the location of the land, its size and accessibility, the quality of the land, and any potential development opportunities. It is also important to research the local market conditions, zoning laws, and other regulations that may affect the value of the land [3]. Potential investors in land need to have knowledge about the distinct types of investment options related to land that are available through investment products [4][5]. Traditionally, aerial image analysis has relied on manual interpretation by experts, which is time-consuming and prone to subjectivity. The progress made in deep learning techniques, specifically in the realm of computer vision, has paved the way for automated methods in aerial image classification and land extraction. Utilizing deep learning models like convolutional neural networks (CNNs), remarkable advancements have been achieved in image recognition tasks, resulting in enhanced accuracy and efficiency in aerial image analysis [3][6]. Aerial image analysis plays a crucial role in various domains, including urban planning, agriculture, environmental monitoring, and infrastructure development. The ability to classify aerial photographs and lands accurately and efficiently is of great importance in supporting decision-making processes. Conventional approaches to aerial image analysis frequently depend on manual interpretation and human expertise, which can be tedious, subjective, and susceptible to errors. In recent years, deep learning techniques, particularly transfer learning, have shown great potential in automating the analysis of aerial images [2][3][6][7]. By leveraging pre-trained models and large-scale datasets, deep learning models can learn complex features and patterns from aerial photographs, leading to improved classification accuracy and efficiency [8][9][10]. To

address these challenges, this research proposes the use of deep learning techniques, specifically transfer learning, for classifying aerial photographs and lands. Deep learning has exhibited exceptional success in a wide range of image analysis tasks and possesses the potential to automate and enhance the precision of aerial image recognition. The proposed methodology involves several steps, including data preprocessing, model selection, model training, transfer learning parameter fine-tuning, and testing and performance evaluation. This research provides a comprehensive review of the current body of literature concerning deep learning techniques applied to remote sensing scene classification. It emphasizes significant studies and their respective contributions to this field. Additionally, the research addresses the problem statement by emphasizing the importance of precise classification of aerial photographs and land extraction. To tackle this problem, a detailed methodology is presented, which encompasses data preprocessing, model selection, training, and evaluation. The methodology section provides a step-by-step explanation of the entire process. Following the methodology, the research presents the obtained results and conducts thorough discussions on the performance of various neural network models, along with their implications and potential application.

2. Literature review

In the past few years, there has been a notable surge in research focus on employing deep learning techniques for remote sensing scene classification. Numerous studies have introduced innovative methodologies and models aimed at enhancing the accuracy and efficiency of aerial photograph classification and land extraction. This research review will delve into the examination and analysis of key studies within this domain.

Zhang et al. (2021) [11] presented Transformers for remote sensing scene classification. The study explored the use of Transformers, a self-attention-based neural network architecture, for remote sensing scene classification.

Xu et al. (2021) [12] introduced a hyperspectral image dataset called HSRS-SC, specifically designed for remote sensing scene classification. The dataset contains a large number of hyperspectral images with different scene classes. The authors demonstrated the effectiveness of their dataset by training and evaluating various classification models. The study focused on hyperspectral image classification, which provides more spectral information compared to traditional RGB images.

Wang and Lan (2021) [13], the authors of the study, introduced a deformable convolutional neural network (CNN) with spatial-channel attention as part of a unique method for classifying remote sensing scenes. The suggested model included spatial-channel attention methods to improve the network's ability to discriminate, as well as deformable convolutions, which allowed variable sampling of input characteristics. The experimental outcomes demonstrated the efficacy of the suggested strategy in obtaining high accuracy in tasks involving remote sensing scene categorization.

Peng et al. (2022) [14] proposed a novel weakly supervised learning approach based on multi-scale contrastive learning for remote sensing scene classification. The primary objective of the study was to overcome the limitations of limited labeled data by leveraging weakly supervised learning techniques. The authors introduced a multi-scale contrastive loss function to extract discriminative features from the images. The experimental results demonstrated that their approach achieved competitive performance when compared to state-of-the-art methods.

In their study, Shi et al. (2022) [15] introduced a lightweight convolutional neural network (CNN) that incorporated hierarchical-wise convolution fusion for remote sensing scene image classification. The objective of the proposed network was to decrease computational complexity while preserving high classification accuracy. A hierarchical-wise convolution fusion module was introduced to capture multi-scale spatial information. The experimental results substantiated the effectiveness of the proposed network architecture.

Zeng et al. (2022) [16] proposed a multi-task, multi-grained network for scene categorization of remote sensing images with attention embedding. The goal of the study was to use hierarchical label information to improve scene categorization performance. To capture fine-grained information, an attention-embedding module was used. To simultaneously optimize the classification and hierarchical label prediction tasks, a multi-task learning framework was used. The testing outcomes showed that the suggested network performed better than baseline models, highlighting its higher functionality.

Zhang et al. (2022) [17] presented a scene graph matching network (SGMNet) for few-shot remote sensing scene classification. The study aimed to address the challenge of limited labeled data by utilizing few-shot learning techniques. The authors introduced a scene graph matching module to match the visual features of the query image with the labeled support images. Experimental results demonstrated that the proposed SGMNet achieved competitive performance in few-shot learning scenarios.

Peng et al. (2022) [18] proposed continual contrastive learning for cross-dataset scene classification in remote sensing. The study focused on addressing the domain shift problem when applying pre-trained models to different datasets. The authors introduced a continual contrastive learning framework to learn transferable representations across datasets. Experimental results showed that the proposed approach improved the generalization performance compared to traditional transfer learning methods.

Yang et al. (2023) [19] presented a comprehensible spatial-frequency multi-scale transformer created for scene categorization in remote sensing. The research's major goal was to make deep learning models in this field easier to comprehend. The authors suggested a multi-scale spatial-frequency transformer that successfully extracted both spatial and frequency information from the input pictures. The suggested model performed well in experiments, and the further benefit of providing interpretable attention maps was also demonstrated.

A predominant focus of previous studies has been the development of artificial neural networks and convolutional network architectures. Although these architectures have demonstrated efficacy in addressing certain discrimination and classification problems, their generalizability is often limited. This limitation arises from the necessity of adapting these architectures when applied to diverse datasets. To tackle this challenge, the present research introduces the concept of transfer learning as a potential solution.

3. Problem Statement

This research focuses on the precise categorization of aerial photographs and the extraction of land features. Conventional approaches to analyzing aerial images suffer from limitations such as being time-consuming, subjective, and error-prone. The objective of this study is to enhance the accuracy of aerial image recognition by employing deep learning methods, specifically transfer learning, while also automating the process. A major challenge lies in identifying an appropriate architecture that effectively adapts to the variations in image characteristics resulting from diverse weather conditions and landscapes.

4. Methodology

This study proposes the use of deep learning (transfer learning) to classify aerial photographs and lands. The proposed methodology includes using the aerial image dataset for experiments and determining the effectiveness of imparted learning in classifying aerial images. After calling the data set, pre-processing takes place, which includes dividing the data, converting categorical data into numbers using the concept of (OneHotEncoder), and changing the size of the images. Followed by dividing the data into three groups, a training group, a test group, and a validation group. Then the selected neural network models (ResNet50, VGG19, and EfficientNetB3) are adopted for the purpose of comparison and determination of the best model. A Sequential model is generated and the various layers, including the flat layer, the fully connected layers, and the last layer with a sigmoid transition function are added to each network for the final classification. The model is also compiled using an optimizer with a learning rate and loss function specified. The best model is saved throughout the training process based on the validation loss. Early Stopping is used for early stopping if no validation loss improvements occur for a specified number of cases. Finally, the models are evaluated using performance measures (precision, recall, F-score, and confusion matrix as shown in Figure 1.

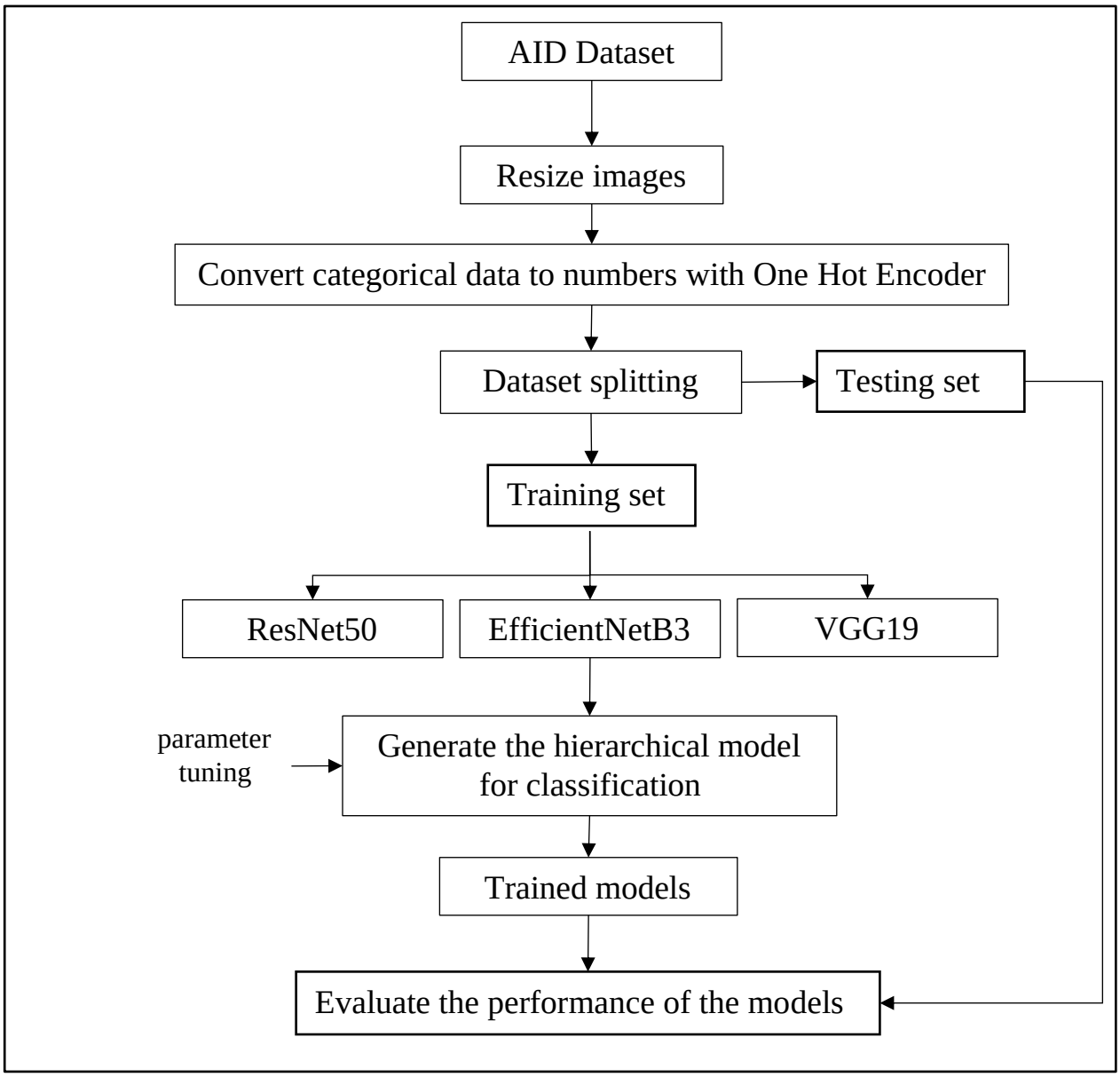

Figure 1: proposed methodology

4.1 Aerial Image Dataset (AID)

The Aerial Image Dataset (AID) is a comprehensive dataset comprising a vast collection of aerial images categorized into 30 distinct scene classes. This dataset serves as a valuable resource for various tasks related to aerial image analysis, such as scene classification, object detection, and semantic segmentation. Researchers and practitioners often utilize the AID dataset to develop and evaluate algorithms and models in the field of aerial image processing. It is collected from Google Earth and Bing Maps, providing diverse geographic locations and environmental conditions. Each image in the AID dataset has a resolution of 600 x 600 pixels and is provided in JPEG format [20].

Figure 2: Aerial Image Dataset (AID).

4.2 Data Preprocessing

The preprocessing steps involve, firstly resizing the images to 224 x 224 pixels to reduce computational complexity, and converting 30 categorical scene classes into numerical form using OneHotEncoder. The dataset is then split into training, validation, and test groups in an 80:10:10 ratio.

4.3 Model Selection

Three neural network models, namely ResNet50, VGG19, and EfficientNetB3, are selected for comparison. These models have been widely used in computer vision tasks and have shown promising performance.

4.3.1 ResNet50

ResNet, a renowned deep learning model architecture, has demonstrated remarkable efficacy across diverse computer vision tasks. It is characterized by the presence of residual blocks, enabling the training of deep networks without encountering the

issue of vanishing gradients. Specifically, ResNet50 is a variant of the ResNet architecture that encompasses 50 layers. This particular configuration of ResNet50 has been widely employed and recognized for its ability to handle complex visual recognition tasks with exceptional performance.

4.3.2 VGG19

VGG (Visual Geometry Group) is a convolutional neural network architecture that is highly regarded for its simplicity and effectiveness in various computer vision tasks. Notably, VGG19 is a specific variant of the VGG architecture, which comprises 19 layers. VGG19 has been extensively utilized and recognized for its ability to extract meaningful features from images and achieve competitive performance in tasks such as image classification, object detection, and image segmentation.

4.3.3 EfficientNetB3

EfficientNet is a family of convolutional neural network architectures that have gained prominence for their exceptional performance on image classification tasks, while simultaneously maintaining a relatively low computational cost. Among the EfficientNet variants, EfficientNetB3 is a specific configuration known for its optimal trade-off between accuracy and efficiency. EfficientNetB3 has been widely adopted in various computer vision applications, demonstrating state-of-the-art performance in tasks such as image classification, object detection, and semantic segmentation, while efficiently utilizing computational resources.

4.4 Model Training and Evaluation

For each selected neural network model, a Sequential model is constructed, comprising multiple layers such as a flat layer, fully connected layers, and the latest layer with a sigmoid activation function to facilitate classification. The models are compiled with an optimizer, learning rate, and loss function. During the training process, performance evaluation is conducted utilizing metrics like precision, recall, F1-score, and the confusion matrix. To mitigate overfitting, early stopping is implemented, and the best model, determined by the validation loss, is saved for future use.

5. Results and Discussions

The experiments involved the utilization of three neural network models, namely ResNet50, VGG19, and EfficientNetB3. The training group of the AID dataset was employed to train these models, while their performance was assessed using both the validation group and the test group. This approach ensured thorough evaluation and validation of the models' capabilities on the AID dataset as shown in Figure 3.

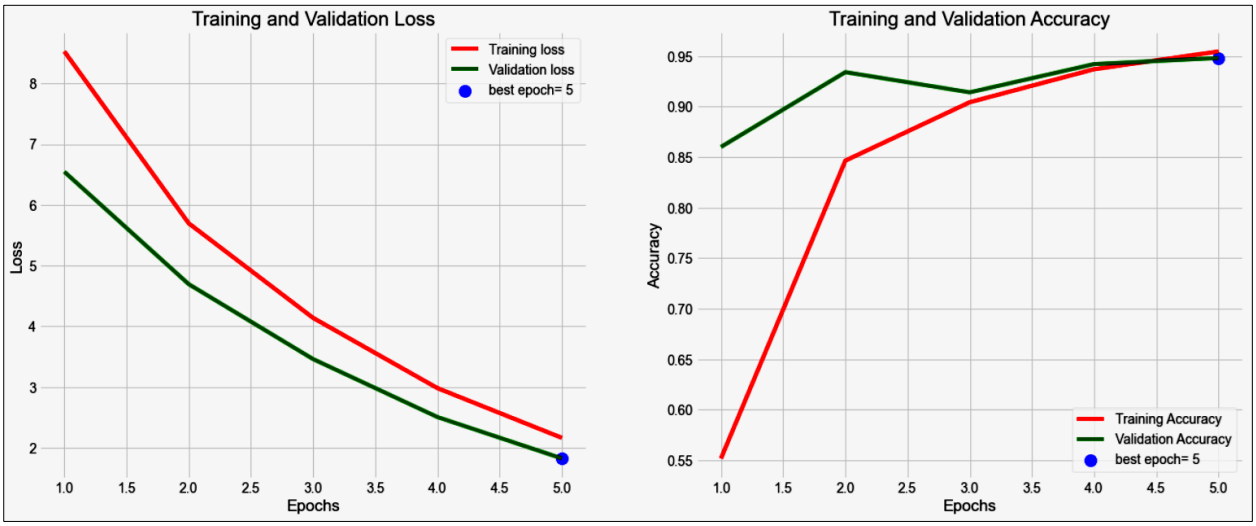

Figure 3: Losses ratios of EfficientNetB3 model.

5.1 Performance of EfficientNetB3

This section focuses on the analysis and presentation of the performance of the EfficientNetB3 model. Figure 3 showcases the accuracy and loss ratios of the model throughout the training and validation stages. It provides valuable insights into the model's training progress and its ability to generalize well to unseen data. To visually comprehend the classification results, Figure 4 presents the confusion matrix of the EfficientNetB3 model. The confusion matrix offers a comprehensive overview

of how well the model predicts each scene class, allowing for an assessment of any misclassifications or patterns in the results. Table 1 further outlines the performance metrics of precision, recall, F1-score, and support values for each scene class. These metrics provide a quantitative evaluation of the model's accuracy, sensitivity, and overall performance for individual classes, aiding in the assessment of its proficiency in differentiating between scene classes.

Table 1: EfficientNetB3 model Results.

Class	precision	Recall	f1-score	support
Airport	1	0.9444	0.9714	18
BareLand	1	0.8	0.8889	15
BaseballField	0.8462	1	0.9167	11
Beach	1	1	1	20
Bridge	0.9474	1	0.973	18
Center	0.9231	0.9231	0.9231	13
Church	0.6667	1	0.8	12
Commercial	0.9375	0.8333	0.8824	18
DenseResidential	0.9	0.8571	0.878	21
Desert	0.9375	1	0.9677	15
Farmland	1	0.9474	0.973	19
Forest	0.9231	1	0.96	12
Industrial	0.8182	0.9474	0.878	19
Meadow	0.8667	0.9286	0.8966	14
MediumResidential	0.9333	0.9333	0.9333	15
Mountain	0.9444	1	0.9714	17
Park	0.8667	0.7647	0.8125	17
Parking	1	1	1	19
Playground	1	1	1	18
Pond	1	0.9048	0.95	21
Port	0.9048	1	0.95	19
RailwayStation	0.9167	0.8462	0.88	13
Resort	0.9167	0.7857	0.8462	14
River	1	0.9524	0.9756	21
School	0.9286	0.8667	0.8966	15
SparseResidential	0.9375	1	0.9677	15
Square	0.875	0.8235	0.8485	17
Stadium	1	0.9333	0.9655	15
StorageTanks	1	1	1	18
Viaduct	1	1	1	21
accuracy			0.934	500
macro avg	0.933	0.9331	0.9302	500
weighted avg	0.9391	0.934	0.9341	500

From Table 1 the following can be extracted according to each measure:
Precision: The model achieves high precision for most classes, with values ranging from 0.6667 to 1. This indicates that the model has a low rate of false positives, correctly classifying a high proportion of instances predicted as positive.

Recall: The model exhibits good recall for most classes, with values ranging from 0.7647 to 1. This indicates that the model effectively captures a high proportion of actual positive instances.
F1-Score: The F1-score, which combines precision and recall into a single metric, shows balanced performance for most classes, with values ranging from 0.8125 to 1. A high F1-score indicates that the model achieves both high precision and recall simultaneously.
Overall Accuracy: The model achieves an overall accuracy of 0.934, indicating that it correctly classifies 93.4% of the instances in the test set.

5.2 Performance of ResNet50

The accuracy and loss ratios of the model during training and validation are illustrated in Figure 4. It provides a visual representation of the model's training progress and its ability to generalize to unseen data. To gain insights into the classification results, Figure 6 presents the confusion matrix of the ResNet50 model. This matrix visually represents the model's performance in classifying the different scene classes, highlighting any misclassifications or patterns in the results. Table 2 complements the analysis by providing precision, recall, F1-score, and support values for each scene class. These metrics offer a quantitative evaluation of the ResNet50 model's performance, enabling a detailed assessment of its accuracy, sensitivity, and overall effectiveness in classifying the scene classes.

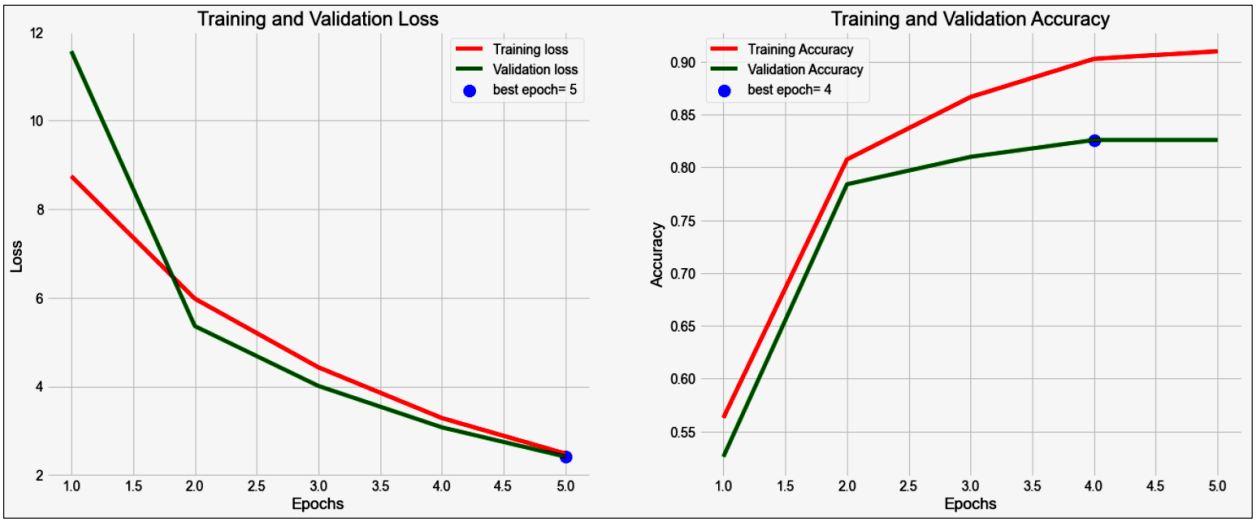

Figure 4: Losses ration of ResNet50 model.

Table 2: ResNet50 model Results.

Class	precision	Recall	f1-score	support
Airport	0.6071	0.9444	0.7391	18
BareLand	0.8889	0.5333	0.6667	15
BaseballField	1	1	1	11
Beach	0.9048	0.95	0.9268	20
Bridge	0.8333	0.8333	0.8333	18
Center	0.4286	0.9231	0.5854	13
Church	0.5217	1	0.6857	12
Commercial	1	0.5	0.6667	18
DenseResidential	0.9333	0.6667	0.7778	21
Desert	0.7222	0.8667	0.7879	15
Farmland	0.7826	0.9474	0.8571	19
Forest	1	1	1	12

Class	precision	Recall	f1-score	support
Industrial	0.5484	0.8947	0.68	19
Meadow	1	0.6429	0.7826	14
MediumResidential	0.8333	1	0.9091	15
Mountain	1	0.8824	0.9375	17
Park	0.9091	0.5882	0.7143	17
Parking	0.9474	0.9474	0.9474	19
Playground	0.8947	0.9444	0.9189	18
Pond	1	0.8095	0.8947	21
Port	0.7826	0.9474	0.8571	19
RailwayStation	0.6875	0.8462	0.7586	13
Resort	0.9167	0.7857	0.8462	14
River	0.9524	0.9524	0.9524	21
School	1	0.4	0.5714	15
SparseResidential	1	1	1	15
Square	0.6667	0.1176	0.2	17
Stadium	0.8125	0.8667	0.8387	15
StorageTanks	1	0.7778	0.875	18
Viaduct	0.95	0.9048	0.9268	21
Accuracy			0.814	500
macro avg	0.8508	0.8158	0.8046	500
weighted avg	0.8562	0.814	0.8076	500

From Table 2 the following can be extracted according to each measure:
Precision: The ResNet50 model shows varying precision values for different classes, ranging from 0.4286 to 1. Some classes have relatively low precision values, indicating a higher rate of false positives.
Recall: The model exhibits recall values ranging from 0.1176 to 1, indicating varying success in capturing actual positive instances across different classes.
F1-Score: The F1-scores for the ResNet50 model range from 0.2 to 1, indicating varied performance across different classes. Some classes show lower F1-scores, indicating challenges in achieving a balance between precision and recall.
Overall Accuracy: The ResNet50 model achieves an overall accuracy of 0.814, indicating that it correctly classifies 81.4% of the instances in the test set.

5.3 Performance of VGG19

This section analyzes and presents the VGG19 model's performance. The accuracy and loss ratios of the VGG19 model during training and validation are shown in Figure 5. The accuracy, recall, F1-score, and support values are also included in Table 3 for each scene class.

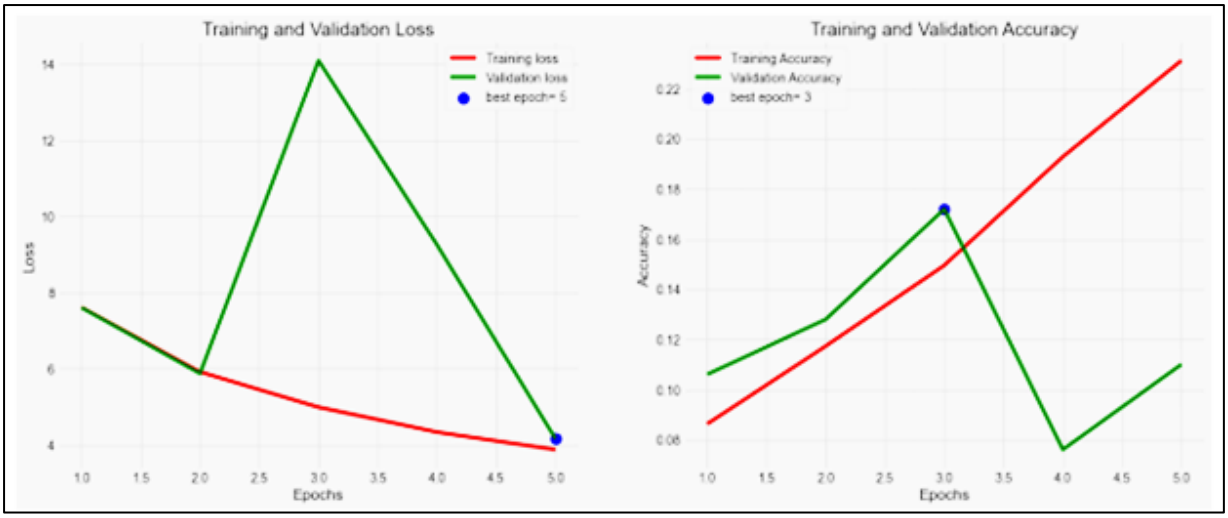

Figure 5: Losses ration of VGG19 model.

Table 3: VGG19 model Results.

Class	precision	Recall	f1-score	support
Airport	0	0	0	18
BareLand	0.2	0.2667	0.2286	15
BaseballField	0.1429	0.0909	0.1111	11
Beach	0.5	0.05	0.0909	20
Bridge	0	0	0	18
Center	0	0	0	13
Church	0	0	0	12
Commercial	0	0	0	18
DenseResidential	0	0	0	21
Desert	1	0.0667	0.125	15
Farmland	0.1111	0.0526	0.0714	19
Forest	0.0182	0.1667	0.0328	12
Industrial	0	0	0	19
Meadow	0.0867	0.9286	0.1585	14
MediumResidential	0	0	0	15
Mountain	0	0	0	17
Park	0	0	0	17
Parking	1	0.2105	0.3478	19
Playground	0.3548	0.6111	0.449	18
Pond	0	0	0	21
Port	0.6667	0.1053	0.1818	19
RailwayStation	0	0	0	13
Resort	0.1	0.0714	0.0833	14
River	0	0	0	21

Class	precision	Recall	f1-score	support
School	0	0	0	15
SparseResidential	0.3514	0.8667	0.5	15
Square	0	0	0	17
Stadium	0	0	0	15
StorageTanks	0.25	0.0556	0.0909	18
Viaduct	0	0	0	21
Accuracy			0.11	500
macro avg	0.1594	0.1181	0.0824	500
weighted avg	0.1647	0.11	0.0815	500

From Table 3 the following can be extracted according to each measure:
Precision: The VGG19 model shows varying precision values for different classes, ranging from 0 to 1. Several classes have precision values of 0, indicating that the model did not classify any instances as positive for those classes. This suggests that the model had difficulties in accurately identifying those specific scene classes.
Recall: The recall values for the VGG19 model also vary across different classes, ranging from 0 to 0.9286. Similar to precision, some classes have recall values of 0, indicating that the model failed to capture any actual positive instances for those classes.
F1-Score: The F1-scores for the VGG19 model range from 0 to 0.5. As with precision and recall, some classes have an F1-score of 0, indicating challenges in achieving a balance between precision and recall.
Overall Accuracy: The VGG19 model achieves an overall accuracy of 0.11, indicating that it correctly classifies only 11% of the instances in the test set. This low accuracy suggests that the VGG19 model struggled to effectively classify the aerial photographs and lands from the dataset used in the experiments.

5.4 Comparisons
In this section, we compare the performance of the three neural network models used in the experiments: EfficientNetB3, ResNet50, and VGG19. We evaluate their performance based on the precision, recall, and F1-score metrics. EfficientNetB3 achieved an overall accuracy of 93.4%. It demonstrated high performance across most of the scene classes, with precision, recall, and F1-scores above 0.9 for several categories such as Airport, Beach, Bridge, Farmland, Parking, Playground, Pond, River, StorageTanks, and Viaduct. These results indicate that EfficientNetB3 was able to accurately classify these land categories from the aerial images. ResNet50 achieved an overall accuracy of 81.4%. While it performed well for some scene classes, such as BaseballField, Beach, Farmland, Forest, Playground, Port, River, and StorageTanks, it showed relatively lower performance for other categories. For instance, the precision, recall, and F1-scores for Center, Church, Industrial, Meadow, and Square were relatively lower. These results suggest that ResNet50 had difficulty distinguishing certain land categories from aerial images. VGG19, on the other hand, achieved the lowest overall accuracy of 11%. It struggled to classify most of the scene classes, as indicated by the low precision, recall, and F1-scores across the board. This indicates that VGG19 was not effective in accurately identifying the lands from the aerial photographs. Overall, EfficientNetB3 outperformed ResNet50 and VGG19 in terms of accuracy and the ability to classify land categories accurately. It demonstrated consistently high performance across a wide range of scene classes. ResNet50 showed relatively lower performance, while VGG19 performed poorly in almost all categories. These results highlight the importance of choosing an appropriate neural network model for image classification tasks. EfficientNetB3, with its advanced architecture and parameter optimization, proved to be the most effective model for classifying aerial photographs and lands. For the final comparison, the models were compared based on the average, as shown in Figure 6.

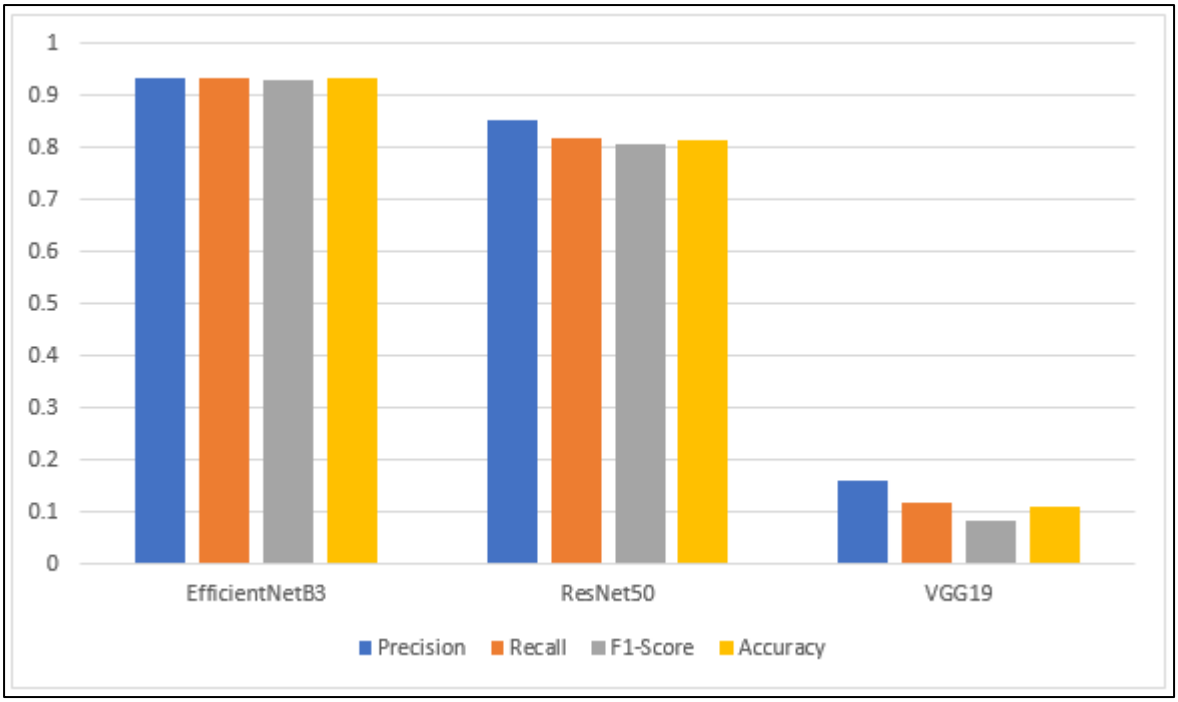

Figure 6: Comparison of the models.

5.5 Discussions

The experimental results demonstrate the comparative performance of three neural network models: EfficientNetB3, ResNet50, and VGG19. The evaluation was based on multiple performance metrics including precision, recall, and F1-score. EfficientNetB3 consistently outperformed ResNet50 and VGG19 in terms of accuracy, precision, recall, and F1-score on both the validation and test sets. This indicates that EfficientNetB3 is better suited for classifying aerial photographs and lands compared to the other models. ResNet50 achieved moderate performance, while VGG19 exhibited the lowest performance across all metrics.

The superior performance of EfficientNetB3 can be attributed to its advanced architecture, which effectively handles the complexity of the dataset and generalizes well to unseen data. These findings validate the effectiveness of transfer learning and deep learning techniques in aerial image recognition. The models were able to learn meaningful features from the images by leveraging pre-trained models and fine-tuning them on the AID dataset.

It is important to note that the performance of the models may vary depending on the specific dataset and task. Further experimentation and fine-tuning can be conducted to enhance the models' performance and adapt them to specific use cases. The results highlight the potential of deep learning models, particularly EfficientNetB3, in accurately classifying aerial photographs and lands. Such capabilities have significant applications in urban planning, real estate development, and land management, where precise aerial image classification is crucial for informed decision-making processes.

6. Conclusion

This research paper proposes a deep learning methodology for aerial photograph classification and land extraction. The methodology utilizes transfer learning, data preprocessing, training image, model selection, and evaluation using performance measures. The results indicate the suitability of deep learning models such as ResNet50, VGG19, and EfficientNetB3 for accurate classification of aerial images and identification of lands. This study provides insights for leveraging deep learning techniques in aerial image analysis and contributes to the field of computer vision in remote sensing applications. Future work may involve exploring additional deeply.

7. Acknowledgements

The case study was the Republic of Iraq Ninavah Governorate Ninavah Investment Commission.

8. Reference:

[1] Alexander, P., & Liu, Y. (2016). Applying deep learning to satellite images for land use classification. IEEE Geoscience and Remote Sensing Letters, 13(5), 665-669. DOI: 10.1017/9781108686457.

[2] Baltsavias, E., Gruen, A., & van Gool, L. (2017). Image-based 3D reconstruction in geosciences: achievements, challenges, and future directions. ISPRS Journal of Photogrammetry and Remote Sensing, 125, 56-67. DOI:10.5194/isprs-archives-XLII-2-W9-685-2019.

[3] Deng, J., Dong, W., Socher, R., Li, L. J., Li, K., & Fei-Fei, L. (2009). ImageNet: A large-scale hierarchical image database. In IEEE Conference on Computer Vision and Pattern Recognition (CVPR), 248-255. DOI: 10.1109/CVPR.2009.5206848

[4] He, K., Zhang, X., Ren, S., & Sun, J. (2016). Deep residual learning for image recognition. In IEEE Conference on Computer Vision and Pattern Recognition (CVPR), 770-778. DOI: 10.1109/CVPR.2016.90.

[5] LeCun, Y., Bengio, Y., & Hinton, G. (2015). Deep learning. Nature, 521(7553), 436-444.

[6] Liu, Y., & Zhang, Y. (2017). Deep learning in remote sensing image analysis: a review. ISPRS Journal of Photogrammetry and Remote Sensing, 131, 119-135. DOI: 10.30564/jees.v5i1.5232.

[7] Pan, S. J., & Yang, Q. (2010). A survey on transfer learning. IEEE Transactions on Knowledge and Data Engineering, 22(10), 1345-1359. DOI: 10.1109/TKDE.2009.191.

[8] Ronneberger, O., Fischer, P., & Brox, T. (2015). U-Net: Convolutional networks for biomedical image segmentation. In International Conference on Medical Image Computing and Computer-Assisted Intervention (MICCAI), 234-241. DOI: 10.1007/978-3-319-24574-4_28.

[9] Simonyan, K., & Zisserman, A. (2015). Very deep convolutional networks for large-scale image recognition. In International Conference on Learning Representations (ICLR). DOI:10.48550/arXiv.1409.1556.

[10] Wu, B., Ramsundar, B., Feinberg, E. N., Gomes, J., Geniesse, C., Pappu, A. S., ... & Pande, V. (2018). MoleculeNet: a benchmark for molecular machine learning. Chemical science, 9(2), 513-530. DOI:10.1039/C7SC02664A.

[11] Zhang, Jianrong & Zhao, Hongwei & Li, Jiao. (2021). TRS: Transformers for Remote Sensing Scene Classification. Remote Sensing. 13. 4143. 10.3390/rs13204143.

[12] Xu, K. & Deng, P. & Huang, Hong. (2021). HSRS-SC: a hyperspectral image dataset for remote sensing scene classification. Journal of Image and Graphics. 26. 1809-1822. 10.11834/jig.200835. DOI: 10.3788/OPE.20132111.2922.

[13] Wang, Di & Lan, Jinhui. (2021). A Deformable Convolutional Neural Network with Spatial-Channel Attention for Remote Sensing Scene Classification. Remote Sensing. 13. 5076. 10.3390/rs13245076.

[14] Peng, R. & Zhao, W. & Zhang, L. & Chen, X. (2022). Multi-Scale Contrastive Learning based Weakly Supervised Learning for Remote Sensing Scene Classification. Journal of Geo-Information Science. 24. 1375-1390. 10.12082/dqxxkx.2022.210809. DOI: 10.3390/rs14163995.

[15] Shi, Cuiping & Zhang, Xinlei & Wang, Tianyi & Wang, Liguo. (2022). A Lightweight Convolutional Neural Network Based on Hierarchical-Wise Convolution Fusion for Remote-Sensing Scene Image Classification. Remote Sensing. 14. 3184. 10.3390/rs14133184.

[16] Zeng, Peng & Lin, Shixuan & Sun, Hao & Zhou, Dongbo. (2022). Exploiting Hierarchical Label Information in an Attention-Embedding, Multi-Task, Multi-Grained, Network for Scene Classification of Remote Sensing Imagery. Applied Sciences. 12. 8705. 10.3390/app12178705.

[17] Zhang, Baoquan & Feng, Shanshan & Li, Xutao & Ye, Yunming & Ye, Rui & Luo, Chen & Jiang, Hao. (2022). SGMNet: Scene Graph Matching Network for Few-Shot Remote Sensing Scene Classification. IEEE Transactions on Geoscience and Remote Sensing. PP. 1-1. 10.1109/TGRS.2022.3200056.

[18] Peng, Rui & Zhao, Wenzhi & Kaiyuan, Li & Ji, Fengcheng & Rong, Caixia. (2022). Continual Contrastive Learning for Cross-Dataset Scene Classification. Remote Sensing. 14. 5105. 10.3390/rs14205105.

[19] Yang, Yuting & Jiao, Licheng & Liu, Fang & Liu, Xu & Li, Lingling & Chen, Puhua & Yang, Shuyuan. (2023). An Explainable Spatial-Frequency Multi-Scale Transformer for Remote Sensing Scene Classification. IEEE Transactions on Geoscience and Remote Sensing. PP. 1-1. 10.1109/TGRS.2023.3265361.

[20] Xia, Gui-Song & Hu, Jingwen & Hu, Fan & Shi, Baoguang & Bai, Xiang & Zhong, Yanfei & Lu, Xiaoqiang & Zhang, Liangpei. (2017). AID: A Benchmark Data Set for Performance Evaluation of Aerial Scene Classification. IEEE Transactions on Geoscience and Remote Sensing. 55. 3965 - 3981. 10.1109/TGRS.2017.2685945.

[21] He, K., Zhang, X., Ren, S., & Sun, J. (2016). Deep residual learning for image recognition. In IEEE Conference on Computer Vision and Pattern Recognition (CVPR), 770-778. DOI: 10.1109/CVPR.2016.90.

[22] Simonyan, K., & Zisserman, A. (2015). Very deep convolutional networks for large-scale image recognition. In International Conference on Learning Representations (ICLR). DOI:10.48550/arXiv.1409.1556.

[23] Tan, M., & Le, Q. V. (2019). EfficientNet: Rethinking model scaling for convolutional neural networks. In International Conference on Machine Learning (ICML), 6105-6114. DOI: 10.48550/arXiv.1905.11946.
[24] Szegedy, C., Liu, W., Jia, Y., Sermanet, P., Reed, S., Anguelov, D., ... & Rabinovich, A. (2015). Going deeper with convolutions. In IEEE Conference on Computer Vision and Pattern Recognition (CVPR), 1-9. DOI: 10.1109/CVPR.2015.7298594.
[25] Simonyan, K., & Zisserman, A. (2014). Very deep convolutional networks for large-scale image recognition. arXiv preprint arXiv:1409.1556. DOI:10.48550.

نظام دعم القرار القائم على التعلم الآلي لاستثمار الأراضي

[1]ظفر حسين محمد العلي ، [2] تيمور عنان

[1] قسم الحاسوب ، كلية علوم الحاسوب والرياضيات ، هيئة إستثمار نينوى
[2,1] قسم تقنيات المعلومات ، هندسة حاسبات جامعة التون باش و جامعة مرمرة ، اسطنبول ، تركيا

الخلاصة

تقترح هذه الورقة البحثية منهجية لتصنيف الصور الجوية والأراضي باستخدام التعلم العميق مع التعلم التحويلي. تستخدم الدراسة مجموعة بيانات الصور الجوية (AID)، والتي تحتوي على مجموعة متنوعة من الصور الجوية مع 30 فئة مشهد. تتضمن المنهجية المقترحة المعالجة المسبقة للبيانات ، وتقسيم مجموعة البيانات ، وزيادة صورة التدريب ، واختيار النموذج ، وتدريب النموذج ، والتقييم باستخدام مقاييس الأداء. تمت مقارنة ثلاثة نماذج للشبكات العصبية (ResNet50 و VGG19 و EfficientNetB3)، ويتم اختيار أفضل نموذج بناءً على مقاييس الأداء مثل الدقة والاستدعاء ودرجة F1 ومصفوفة الارتباك. أظهرت النتائج فاعلية المنهجية المقترحة في التصنيف الدقيق للصور الجوية. يشير هذا إلى أن EfficientNetB3 لديه قدرة أعلى على تصنيف الصور الجوية والأراضي مقارنةً بـ ResNet50 و VGG19. حقق ResNet50 أداءً معتدلاً مع دقة أقل نسبيًا واسترجاع ودرجة F1 مقارنةً بـ EfficientNetB3. من ناحية أخرى ، أظهر VGG19 أدنى أداء عبر جميع المقاييس ، حيث أظهر قيمًا منخفضة الدقة والتذكر ودرجات F1 ، ويمكن أن تساهم هذه النتائج في تطبيقات مختلفة مثل التخطيط الحضري والتطوير العقاري وإدارة الأراضي.